LETTER • OPEN ACCESS

Elucidating the present-day chemical composition, seasonality and source regions of climate-relevant aerosols across the Arctic land surface

View the article online for updates and enhancements.

You may also like

ENVIRONMENTAL RESEARCH
LETTERS

LETTER

Elucidating the present-day chemical composition, seasonality and source regions of climate-relevant aerosols across the Arctic land surface

Vaios Moschos[1] , Julia Schmale[1,2] , Wenche Aas[3] , Silvia Becagli[4,5], Giulia Calzolai[6] , Konstantinos Eleftheriadis[7] , Claire E Moffett[8], Jürgen Schnelle-Kreis[9], Mirko Severi[4,5], Sangeeta Sharma[10], Henrik Skov[11], Mika Vestenius[12], Wendy Zhang[10], Hannele Hakola[12], Heidi Hellén[12], Lin Huang[10] , Jean-Luc Jaffrezo[13], Andreas Massling[11], Jakob K Nøjgaard[14], Tuukka Petäjä[15], Olga Popovicheva[16], Rebecca J Sheesley[8], Rita Traversi[4,5], Karl Espen Yttri[3], André S H Prévôt[1], Urs Baltensperger[1] and Imad El Haddad[1]

1 Laboratory of Atmospheric Chemistry, Paul Scherrer Institute, Villigen-PSI, Switzerland
2 Extreme Environments Research Laboratory, École Polytechnique Fédérale de Lausanne, Lausanne, Switzerland
3 NILU—Norwegian Institute for Air Research, Kjeller, Norway
4 Department of Chemistry 'Ugo Schiff', University of Florence, Florence, Italy
5 Institute of Polar Sciences, ISP-CNR, Venice-Mestre, Italy
6 National Institute for Nuclear Physics (INFN), Florence division, Florence, Italy
7 Environmental Radioactivity Laboratory, NCSR Demokritos, Athens, Greece
8 Department of Environmental Science, Baylor University, Waco, TX, United States of America
9 Joint Mass Spectrometry Centre, Helmholtz Zentrum München, München, Germany
10 Climate Research Division, Environment and Climate Change Canada, Toronto, Canada
11 Department of Environmental Science, iClimate, Aarhus University, Roskilde, Denmark
12 Atmospheric Composition Research, Finnish Meteorological Institute, Helsinki, Finland
13 Institute of Environmental Geosciences, University Grenoble Alpes, CNRS, Grenoble, France
14 The National Research Centre for the Working Environment, Copenhagen, Denmark
15 Institute for Atmospheric and Earth System Research/Physics, University of Helsinki, Helsinki, Finland
16 Skobeltsyn Institute of Nuclear Physics, Lomonosov Moscow State University, Moscow, Russia

E-mail: julia.schmale@epfl.ch and imad.el-haddad@psi.ch

Abstract

The Arctic is warming two to three times faster than the global average, and the role of aerosols is not well constrained. Aerosol number concentrations can be very low in remote environments, rendering local cloud radiative properties highly sensitive to available aerosol. The composition and sources of the climate-relevant aerosols, affecting Arctic cloud formation and altering their microphysics, remain largely elusive due to a lack of harmonized concurrent multi-component, multi-site, and multi-season observations. Here, we present a dataset on the overall chemical composition and seasonal variability of the Arctic total particulate matter (with a size cut at 10 μm, PM_{10}, or without any size cut) at eight observatories representing all Arctic sectors. Our holistic observational approach includes the Russian Arctic, a significant emission source area with less dedicated aerosol monitoring, and extends beyond the more traditionally studied summer period and black carbon/sulfate or fine-mode pollutants. The major airborne Arctic PM components in terms of dry mass are sea salt, secondary (non-sea-salt, nss) sulfate, and organic aerosol (OA), with minor contributions from elemental carbon (EC) and ammonium. We observe substantial spatiotemporal variability in component ratios, such as EC/OA, ammonium/nss-sulfate and OA/nss-sulfate, and fractional contributions to PM. When combined with component-specific back-trajectory analysis to identify marine or terrestrial origins, as well as the companion study by Moschos *et al* 2022 *Nat. Geosci.* focusing on OA, the composition analysis provides policy-guiding observational insights into sector-based differences in natural and

anthropogenic Arctic aerosol sources. In this regard, we first reveal major source regions of inner-Arctic sea salt, biogenic sulfate, and natural organics, and highlight an underappreciated wintertime source of primary carbonaceous aerosols (EC and OA) in West Siberia, potentially associated with the oil and gas sector. The presented dataset can assist in reducing uncertainties in modelling pan-Arctic aerosol-climate interactions, as the major contributors to yearly aerosol mass can be constrained. These models can then be used to predict the future evolution of individual inner-Arctic atmospheric PM components in light of current and emerging pollution mitigation measures and improved region-specific emission inventories.

1. Introduction

The rapidly changing Arctic environment is characterised by a substantial sea ice loss and land surface temperature increase at a rate of 0.5 °C per decade since the late 1970s (IPCC 2013, 2021). This world's highest rate of warming is called Arctic amplification (Serreze and Barry 2011, Block *et al* 2019), and is driven primarily by the greenhouse gas (e.g. CO_2) forcing, the Planck feedback, and the snow and ice albedo effect (Pithan and Mauritsen 2014, Hegerl *et al* 2019), as well as low-level clouds (e.g. Curry and Ebert 1992, Shupe and Intrieri 2004, Lubin and Vogelmann 2006, Tan and Storelvmo 2019). The warming is accompanied by changing inner-Arctic natural and anthropogenic particulate matter (PM, or aerosol) and precursor emissions due to environmental and socio-economic change (Kirkevåg *et al* 2013, Schmale *et al* 2018).

Short-lived particulate climate forcers are estimated to exert an annual-mean net-cooling direct radiative effect in the Arctic (Sand *et al* 2015). The observed long-term trends in the single scattering albedo at different Arctic stations indicate significant spatial variability (Collaud Coen *et al* 2020), which remains to be elucidated in terms of PM chemical composition to resolve the sources. The recent combined decline in (scattering) sulfate and (absorbing) black/elemental carbon (BC/EC) aerosols (Schmale *et al* 2021a), due to better emission regulations across the Arctic Council nations, might explain a non-negligible fraction of the Arctic surface warming (Acosta Navarro *et al* 2016, Dobricic *et al* 2019, Ren *et al* 2020). Still, there is a particular need to understand which sources reduce both absorbing aerosols (e.g. BC/EC) and long-lived greenhouse gases (Shindell and Faluvegi 2009, AMAP 2015, Najafi *et al* 2015, Lohmann *et al* 2020). Further, a significant aspect of the Arctic aerosol impacts on climate is their influence on the Arctic sea ice through interference with the Arctic clouds and radiation (Wang *et al* 2018). Hence, the question of whether potential short-term mitigation actions can result in a climate benefit, i.e. net Arctic cooling (Sand *et al*

2015), can only be answered if also the highly variable Arctic aerosol-cloud effects (Liu and Key 2014) are better understood in terms of sign and magnitude. That is because the indirect effect is likely more important than the direct effect in the Arctic (Menon *et al* 2008, Struthers *et al* 2011), where the limited amount of available aerosol can constrain cloud formation (Mauritsen *et al* 2011). The post-Soviet industrial collapse is associated with a decrease in inner-Arctic anthropogenic emissions over the past decades (Sirois and Barrie 1999, Laing *et al* 2013, Kyrö *et al* 2014, Sharma *et al* 2019). However, aerosol concentrations remain less monitored in the vast Siberian Arctic (Popovicheva *et al* 2017, 2019, Manousakas *et al* 2020), a region listed among the four global observational hot spots with limited spatial coverage (Kulmala 2018). Models simulate aerosol-climate effects with low confidence at high northern latitudes (i.e. large inter-model spread), owing to a lack of extensive, spatially-resolved observational constraints (Mann *et al* 2014, Arnold *et al* 2016, Sand *et al* 2017, Willis *et al* 2018, Petäjä *et al* 2020, Schmale *et al* 2021b). That can lead to biased regional or global warming estimates (IPCC 2013, Cohen *et al* 2014, Yang *et al* 2014, Cohen *et al* 2018).

Knowing the pan-Arctic yearly aerosol loading and chemical composition is crucial, as their future changes will impact the radiative balance of the Arctic atmosphere, whereby the net cooling or warming effect at different sites and seasons remains uncertain (Wegmann *et al* 2018, Schmale *et al* 2021b). The aerosol-climate effects, i.e. direct absorption or scattering of solar radiation, the cloud condensation nuclei (CCN) and ice nucleation activity, and therewith impact on the indirect aerosol effect, are a function of the aerosol chemical composition, particle size, and mixing state (Nguyen *et al* 2017, Adachi *et al* 2021), because different components have different physicochemical properties. Those properties lead to different optical characteristics (absorbing and scattering potential) and different hygroscopicity or ice-nucleating abilities relevant to aerosol-cloud-climate interactions (Liu and Wang 2010, Lange *et al* 2019, Schneider *et al* 2021). In addition, compound

volatility and acidity (e.g. Wang *et al* 2020) are critical for multiphase chemical reactions that ultimately determine many physicochemical properties (Wang *et al* 2020, Tong *et al* 2021). While enhanced observational and modelling efforts for Arctic atmospheric BC and its deposition have been conducted (Qian *et al* 2014, Cho *et al* 2019, Winiger *et al* 2019), the Arctic organic aerosol (OA) mass and its importance relative to EC or inorganic aerosols are still poorly characterised (Uttal *et al* 2016). Major ions such as sulfate, nitrate, and ammonium, are routinely monitored at several Arctic stations. However, beyond those, not all the different key aerosol components and concentration trends are observed together and in sufficient detail to reduce uncertainties in aerosol-climate interaction simulations (Quinn *et al* 2007, Hirdman *et al* 2010). So far, many studies were only able to develop a limited scope, i.e. focus on a small number of sites, a limited number of seasons, or only specific components (Willis *et al* 2018).

Here we present an unprecedented dataset of speciated PM in the recent past from eight sites across all sectors of the Arctic. We have achieved that with a combination of major inorganic ion and EC measurements, as well as offline aerosol mass spectrometry (AMS) analysis (Daellenbach *et al* 2016) for OA quantification and the apportionment of its natural and anthropogenic sources (Moschos *et al* 2022). We emphasise how the different Arctic aerosol components behave relative to each other, how they change over a seasonal cycle and between stations in relative terms, and discuss the assets of the presented pan-Arctic aerosol dataset for simulating future Arctic climate.

2. Method

2.1. Filter sampling and measurements

Filter sampling and subsequent offline measurements have three main advantages: (a) extending the spatial and temporal coverage of the sampled aerosol, as filters are routinely collected at many stations; (b) collection of sufficient aerosol loading to increase the signal-to-noise ratio of subsequent analyses; (c) possibility to analyze the total aerosol including the coarse size fraction (>2.5 μm). We provide an overview of the sampling sites in table 1, including the station acronyms, coordinates and altitude, duration of the sampling, and polar night/midnight sun periods. We collected PM_{10} (particulate matter with an equivalent aerodynamic diameter of less or equal to 10 μm) and total suspended particulate (TSP) matter, i.e. total aerosol without a defined size cut, on quartz fiber filters at the different sites following procedures described elsewhere (Moschos *et al* 2022). We then measured the samples with various offline techniques as outlined below. The typical filter-composite sample time resolution is weekly (more variable at BAR), except for ALT (bi-weekly) and TIK ($\sim$3 d).

We quantified elemental and organic carbon (Sunset OC-EC analyzer-based) by thermal-optical analysis using the EUSAAR-2 protocol (Cavalli *et al* 2010), except for ALT (ECT9; Huang *et al* 2021) and UTQ (NIOSH 5040 protocol). We measured major water-soluble inorganic ionic components (SO_4^{2-}, NO_3^-, Cl^-, NH_4^+, Na^+, K^+, Ca^{2+}, Mg^{2+}) by ion chromatography (Jaffrezo *et al* 1998); ion data for BAR, TIK, and UTQ were presented in Popovicheva *et al* (2019), Manousakas *et al* (2020), and Moffett *et al* (2020), respectively. We measured major ions in samples from ALT during 2018 at two different laboratories, and the measurements and seasonal trends were reproducible (major ions sum: slope = 1.15; R^2 = 0.98; intercept = 0). For all samples, we calculated the ionic balance (in nEq m^{-3}; nEq: nano-equivalents) considering all major inorganic ionic components. We calculated the non-sea-salt (nss) sulfate and sea salt concentrations as follows: $[nss - SO_4^{2-}] = [SO_4^{2-}]–0.252 \times [Na^+]$ and $[Sea\text{-}salt] = [Cl^-] + [Na^+] \times 1.47$, respectively, where the value of 0.252 represents the mass ratio of sulfate-to-sodium in seawater, and 1.47 accounts for the presence of anions and cations other than Na^+ and Cl^- in sea salt (Moffett *et al* 2020). Negative nss-sulfate concentrations were calculated for 2% of the samples but were not significantly different from zero (within measurement errors); we have not considered these samples for calculating the NH_4^+/nss-sulfate and OA/nss-sulfate ratios (outliers). Further, the Cl^-/Na^+ mass ratio was greater than that of seawater (1.8) in only 2 % of the samples, but this value never exceeded 2.1. Our calculations do not include (Na^+-containing) mineral dust, which may become important in long-range episodic air mass transport events or locally (Groot Zwaaftink *et al* 2016). That is because mineral dust is a complex (and variable) mixture of oxides and carbonates and consists of elements that our techniques could not quantify, and none of the measured water-soluble ions can be considered unique tracers for dust. While Ca^{2+} has been used as a tracer to identify air masses influenced by dust, we could not retrieve accurate estimates of dust contribution to PM due to the variability in the Ca^{2+}/total_dust_PM. Our yearly-average Ca^{2+} concentration of 43 ng m^{-3} at ALT is comparable to earlier results for the same station (Sharma *et al* 2019).

As detailed in Moschos *et al* (2022), we utilised a high-resolution long time-of-flight Aerodyne aerosol mass spectrometer (L-ToF-AMS) with electron impact ionisation, for the bulk chemical characterisation of the pan-Arctic OA fraction upon water extraction. We used the AMS OA mass spectra as inputs in positive matrix factorisation (PMF) analysis and the total OA mass was apportioned to different primary vs. secondary and natural vs. anthropogenic source components (Moschos *et al* 2022). Here we focus on the AMS-PMF-based total OA mass

Table 1. Arctic station acronyms, coordinates, altitude (meters above sea level, m asl), polar night and midnight sun periods, sampling period, size cut, and the number of filter sample composites.

Station, country	Acronym	Coordinates	Altitude (m asl)	Polar night	Midnight sun	Sampling period	Size cut	No. samples
Alert, Canada	ALT (A)	82°3′N 62°2′W	210	Oct. 14— Feb. 28	Apr. 07— Sep. 04	Apr'15— Dec'18	None	37
Baranova, Russia	BAR (B)	79°2′N 101°5′E	30	Oct. 22— Feb. 22	Apr. 22— Aug. 22	Apr'15— Nov'16	10 μm	19
Gruvebadet, Norway	GRU (G)	78°9′N 11°9′E	50	Dec. 10— Jan. 22	Apr. 27— Jul. 17	Mar'17— Aug'18	10 μm	20
Pallas, Finland	PAL (P)	68°0′N 24°2′E	340	Nov. 19— Jan. 24	May 11— Aug. 03	Aug'18— Aug'19	10 μm	21
Tiksi, Russia	TIK (T)	71°6′N 128°9′E	20	Nov. 19— Jan. 23	May 11— Aug. 01	Sep'14— Sep'16	None	9
Utqiagvik, USA	UTQ (U)	71°2′N 156°4′W	10	Oct. 16— Feb. 25	Apr. 09— Sep. 02	Jun'16— Aug'17	None	23
Villum, Greenland	VRS (V)	81°4′N 16°4′W	24	Oct. 26— Feb. 15	Apr. 20— Aug. 20	Dec'17— Dec'18	10 μm	23
Zeppelin, Norway	ZEP (Z)	78°5′N 11°5′E	475	Oct. 14— Feb. 28	Apr. 07— Sep. 04	Jan'17— Dec'18	10 μm	22

(OC and heteroatoms mass, WSOC-based), the total anthropogenic OA (Anthr-OA), and methanesulfonic acid-related OA (MSA-OA). We hereafter refer to PM as the sum of the sea salt, ammonium, nitrate, nss-sulfate, EC, and total OA mass concentrations.

2.2. Back-trajectory analysis to identify source regions of aerosol components

Back-trajectories (BTs) show the air mass history (origin and atmospheric transport paths) and thus can provide information on the geographic location of potentially advected emissions at large geographical scales. We performed BT analysis to assess potential source locations of individual Arctic aerosol components over the entire sampling period at each station. We calculated the trajectories backward for 10 d (every 6 h) using the HYSPLIT4 model with meteorological data from the Global Data Assimilation System with one-degree resolution. We weighted the calculated BTs with the time series of each component using the concentration-weighted trajectory (CWT) approach to localise air parcels responsible for high concentrations at the receptor site (Rai *et al* 2020). We used the Igor-based user interface ZeFir (Petit *et al* 2017) to calculate component-specific CWT maps separately for each specific station. The CWT value of a particular grid cell (i, j) (latitude, longitude) is a measure of the source strength of a grid cell to a receptor site and is determined as follows: $\text{CWT}_{ij} = \sum_{l=1}^{L} C_l \tau_{ijl} / \sum_{l=1}^{L} \tau_{ijl}$, where C_l is the concentration corresponding to the arrival of BT l, τ_{ijl} is the number of trajectory segment endpoints in grid cell (i, j) for back trajectory l divided by the total number of trajectory segment endpoints for back trajectory l (i.e. residence time of a trajectory in each grid cell), and L is the total number of back trajectories over the entire period for one station. Since the temporal resolution is low,

enlarging the size of the input dataset, which is a novel tool available in ZeFir, allowed to take more BTs into account and improve their statistical representativeness (Petit *et al* 2017). For instance, when the filter composite time resolution was weekly on average, all trajectories arriving at the station (with a frequency of four times a day) for 7 d back in time since the sampling end (i.e. 7 d temporal extension of the input data) were considered for each sample. We merged results from the CWT-based BT analysis for each Arctic station (without prior normalisation) to highlight component-specific pan-Arctic hot spot source regions, i.e. associated with the highest mass concentrations across all stations, with greater accuracy than would be possible with single-site only results (Han *et al* 2007, Petit *et al* 2017, Moschos *et al* 2022). We combined N-site trajectory analyses (multi-site CWT, MS-CWT) based on the following notation: $\text{MS}-\text{CWT}_{ij} = \sum_{n=1}^{N} \left(\sum_{l=1}^{L} C_{l,n} \tau_{ijln} / \sum_{l=1}^{L} \tau_{ijln} \right) / N$ (Masiol *et al* 2020). TIK was not considered for the BT analysis here, as only a few samples were available with PM measurements, and hence a robust result was less likely to be obtained.

3. Results and discussion

The major aerosol components, in descending order of pan-Arctic relative contributions to PM_{10} and TSP mass (figure 1), are sea salt, secondary (nss) sulfate, OA, ammonium, EC, and nitrate. Considering all measurements, the mean PM mass is 1.6 μg m^{-3} (1st and 3rd quartiles, Q_1–Q_3 = 0.68–2.1 μg m^{-3}). We note that the general composition (and climate effects) of PM_1 and $PM_{2.5}$ might differ. We present individual component yearly mass concentrations in figure S1 (available online at
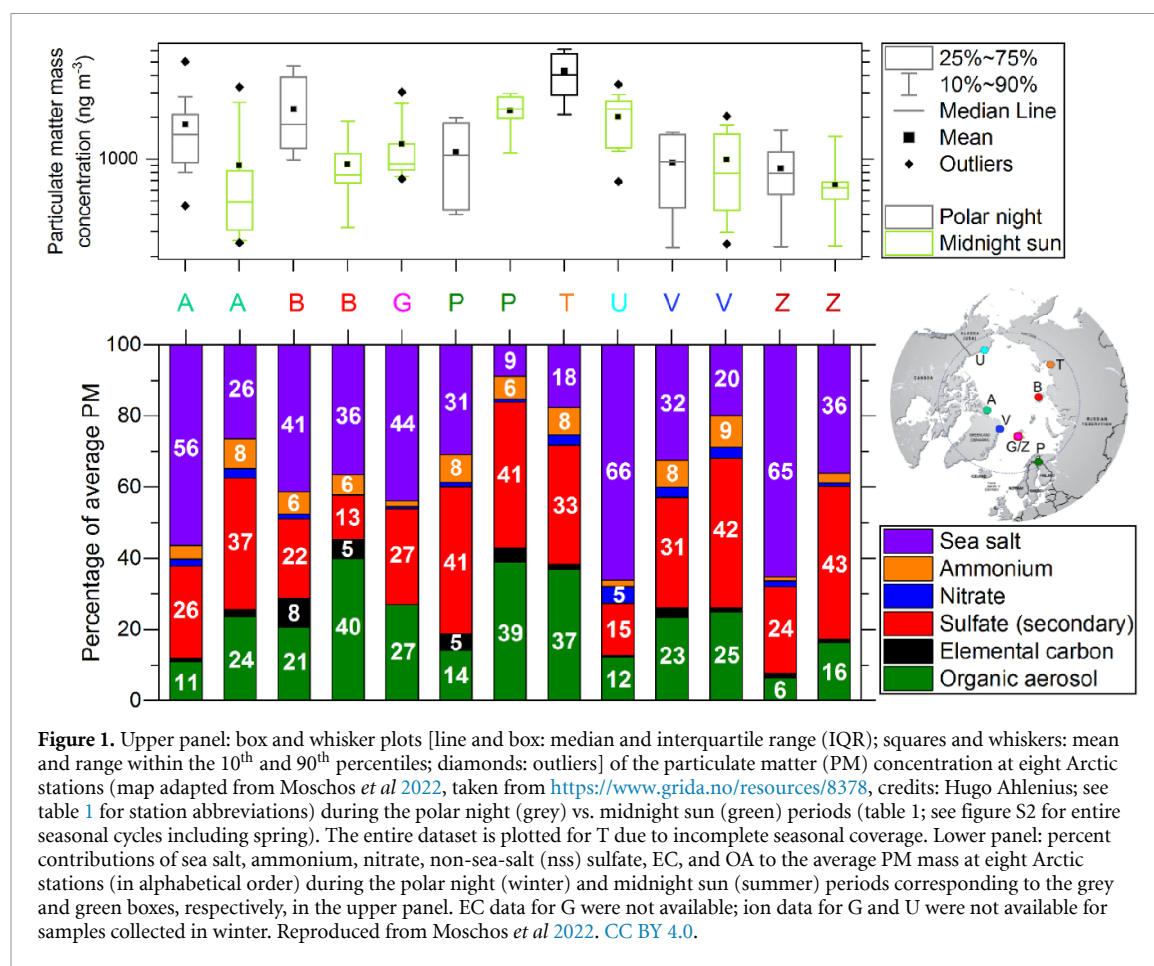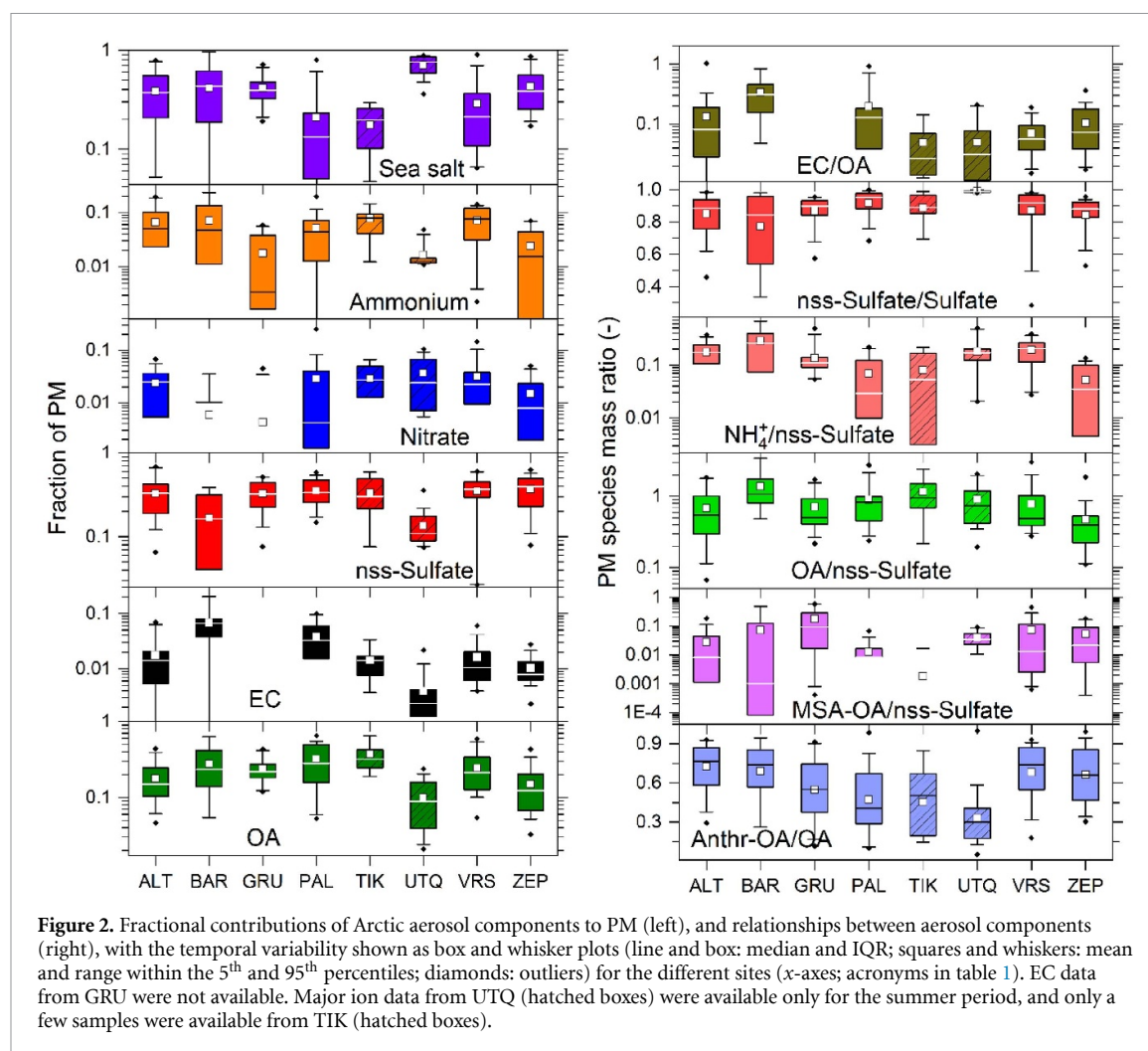
Figure 1. Upper panel: box and whisker plots [line and box: median and interquartile range (IQR); squares and whiskers: mean and range within the 10th and 90th percentiles; diamonds: outliers] of the particulate matter (PM) concentration at eight Arctic stations (map adapted from Moschos *et al* 2022, taken from https://www.grida.no/resources/8378, credits: Hugo Ahlenius; see table 1 for station abbreviations) during the polar night (grey) vs. midnight sun (green) periods (table 1; see figure S2 for entire seasonal cycles including spring). The entire dataset is plotted for T due to incomplete seasonal coverage. Lower panel: percent contributions of sea salt, ammonium, nitrate, non-sea-salt (nss) sulfate, EC, and OA to the average PM mass at eight Arctic stations (in alphabetical order) during the polar night (winter) and midnight sun (summer) periods corresponding to the grey and green boxes, respectively, in the upper panel. EC data for G were not available; ion data for G and U were not available for samples collected in winter. Reproduced from Moschos *et al* 2022. CC BY 4.0.

stacks.iop.org/ERL/17/034032/mmedia) for the different stations. The seasonal cycles of PM (figure S2) reveal that mass concentrations in spring, and in certain cases also during the polar night (winter) period (e.g. at ALT and BAR; figure 1), are usually higher than in summer (midnight sun period). By contrast, biogenic emissions contribute significantly to the higher abundance of PM in summer vs. winter at PAL (Moschos *et al* 2022). Figures 2 and 3 show the relationships between different inorganic and carbonaceous aerosol components and their fractional contributions to PM, as well as their seasonality and spatial variability. We display the BT analysis results for major Arctic aerosol components in figure 4. The findings shown in figures 1–4 are discussed in the following for each chemical component individually.

Sea salt is the major contributor to PM (figure 1) with a mean pan-Arctic contribution to PM (figure 2) of 39% (Q_1–$Q_3 = 19\%$–58%) and an annual mean concentration (figure S1) of 530 ng m^{-3} (Q_1–$Q_3 = 150$–700 ng m^{-3}). At PAL, TIK, and VRS, where the OA and/or nss-sulfate contributions are elevated, the fraction of sea salt is less dominant, i.e. contributing on average 24% of the PM (Q_1–$Q_3 = 8\%$–29%). Elevated relative contributions are observed typically from October to February (figure 3), while absolute concentrations are quite similar across the different

stations (except for PAL and UTQ; figure S1), peaking in November–March (figure S2). For this natural Arctic aerosol component, open ocean (breaking waves), open sea ice fractures, blowing snow, and frost flower fragments are likely sources (Huang and Jaeglé 2017, Kirpes *et al* 2019). Our annual BT analysis demonstrates the marine origin (open ocean or sea ice) of sea salt from the Beaufort, Kara, Laptev, and Chukchi Sea, as well as the Arctic Ocean (figure 4). The sea salt seasonality and major source regions differ from those of MSA-OA, which appears only in summer and originates from the open ocean mainly around the Greenland Sea (Moschos *et al* 2022). Combined, these observations suggest the importance of blowing snow or open sea ice fractures as predominant sea salt sources in winter. That does not preclude significant contributions from the open ocean in summer, for instance at UTQ (figure S3), as indicated by the non-negligible sea salt concentrations throughout the year at multiple stations (figure S1).
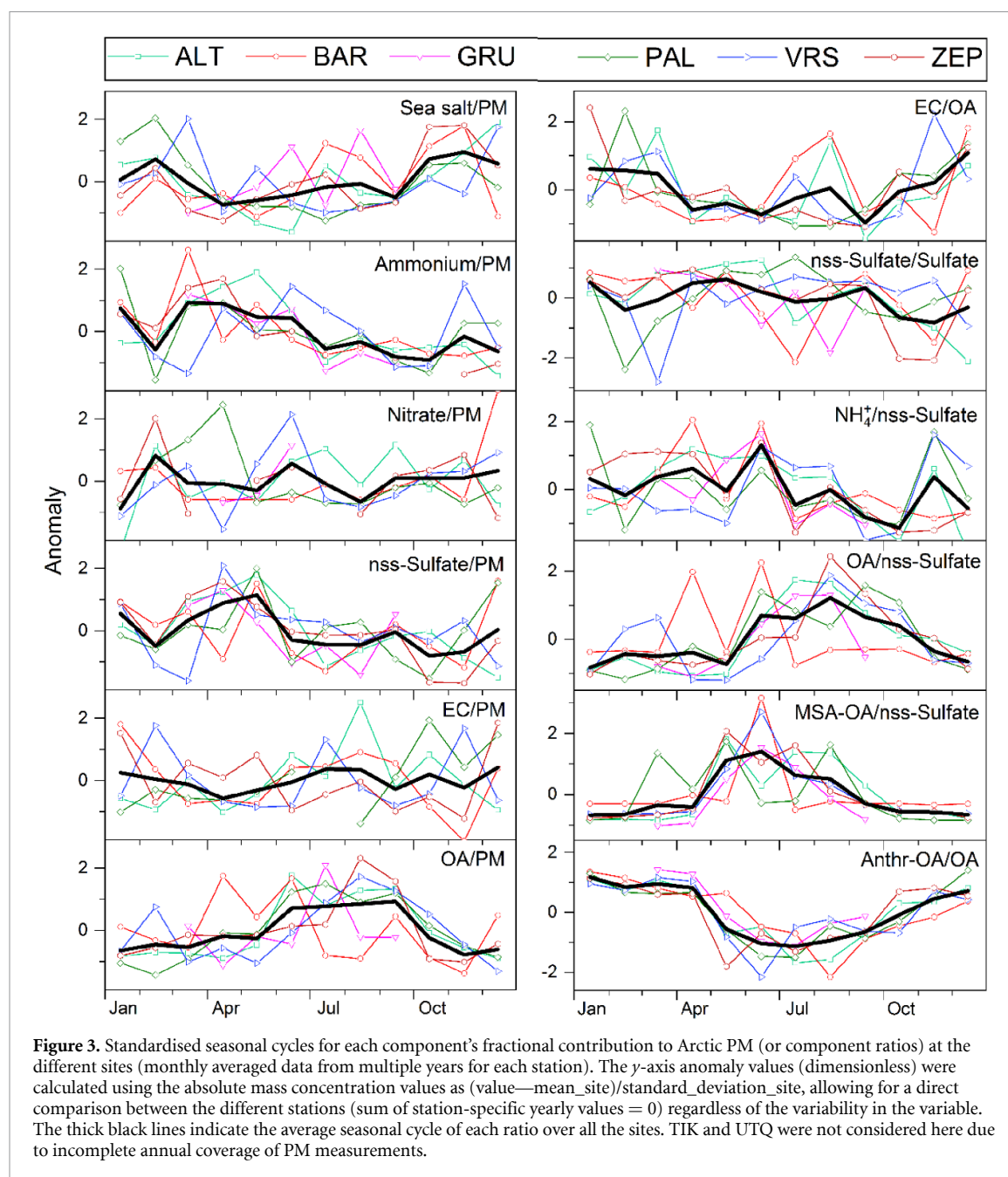
Nss-sulfate contributes on average 30% (Q_1–$Q_3 = 17\%$–41%) to PM across the stations (figure 2). The corresponding annual mean concentration (figure S1) of 470 ng m^{-3} (Q_1–$Q_3 = 160$–630 ng m^{-3}) is similar to reported values at ALT and UTQ (Quinn *et al* 2002, Leaitch *et al* 2018), although these values have been decreasing over the past

Figure 2. Fractional contributions of Arctic aerosol components to PM (left), and relationships between aerosol components (right), with the temporal variability shown as box and whisker plots (line and box: median and IQR; squares and whiskers: mean and range within the 5th and 95th percentiles; diamonds: outliers) for the different sites (x-axes; acronyms in table 1). EC data from GRU were not available. Major ion data from UTQ (hatched boxes) were available only for the summer period, and only a few samples were available from TIK (hatched boxes).

decades (Sharma *et al* 2019, Ren *et al* 2020, Schmale *et al* 2021a). While the nss-sulfate concentrations are largely spatially homogeneous (figure S1) and are thus likely related to regional processes, we observe slightly higher mean values at the Eurasian sites GRU and PAL ($\sim$600 ng m^{-3}), and additional nss-sulfate sources might exist at TIK (1600 ng m^{-3}). The majority of sulfate, typically 80%–90%, is of non-sea-salt origin (figure 2) and associated with the oxidation of SO_2 (i.e. sulfate is secondary), which is of natural (emissions from marine biota) or anthropogenic (fuel combustion) origin, whereas crustal contributions are small (Udisti *et al* 2016). The highest nss-sulfate concentrations ($\sim$1.5 μg m^{-3}; figure 4) are observed in the second half of the Arctic haze period (figure S2) and are associated with air masses arriving from the larger Eurasian region (figure 4), similar to secondary anthropogenic-dominated organics (Moschos *et al* 2022). Hence, the pan-Arctic nss-sulfate is likely predominantly anthropogenic, consistent with past observations at GRU in spring (Udisti *et al* 2016) and yearly and long-term sulfur isotope measurements at ALT (Li and Barrie 1993, Norman *et al* 1999). Based on the BT analysis results, marine source regions of biogenic nss-sulfate can be inferred (figure 4).

The source regions of NH_4^+ (figure 4), which exhibits relatively high (and comparable) concentrations at ALT, BAR, PAL, and highest at TIK (figure S1), are similar to those of nss-sulfate. That indicates the frequent co-emission and conversion of their precursors to ammonium (bi-)sulfate, at least during the peak haze (spring) period (figure S2). Ammonium measurements at such low concentration levels (figure S1; Q_1–Q_3 = 15–100 ng m^{-3}) can be prone to positive artefacts and hence are associated with substantial uncertainties (Xu *et al* 2020). Nevertheless, we derive a pan-Arctic mean ammonium/nss-sulfate ratio (figure 2) of 0.15 (median: 0.12; Q_1–Q_3 = 0.06–0.21), indicating that ammonium is not sufficiently present to neutralise nss-sulfate ($\sim$0.4 in terms of equivalent ratio). When taking all measured major inorganic ions into account, the pan-Arctic ratio of cations-to-anions is 0.9–1.0 (table S1), resulting in a neutral PM$_{10}$ and TSP aerosol. An exception is the station GRU, where the PM might be slightly acidic in many samples (average cations/anions <0.75; table S1) if experimental errors are not accounted for. The significant presence of Na$^+$, originating mainly from sea salt particles, contributes substantially to the near-equal abundance of anions and cations. That

Figure 3. Standardised seasonal cycles for each component's fractional contribution to Arctic PM (or component ratios) at the different sites (monthly averaged data from multiple years for each station). The *y*-axis anomaly values (dimensionless) were calculated using the absolute mass concentration values as (value—mean_site)/standard_deviation_site, allowing for a direct comparison between the different stations (sum of station-specific yearly values = 0) regardless of the variability in the variable. The thick black lines indicate the average seasonal cycle of each ratio over all the sites. TIK and UTQ were not considered here due to incomplete annual coverage of PM measurements.
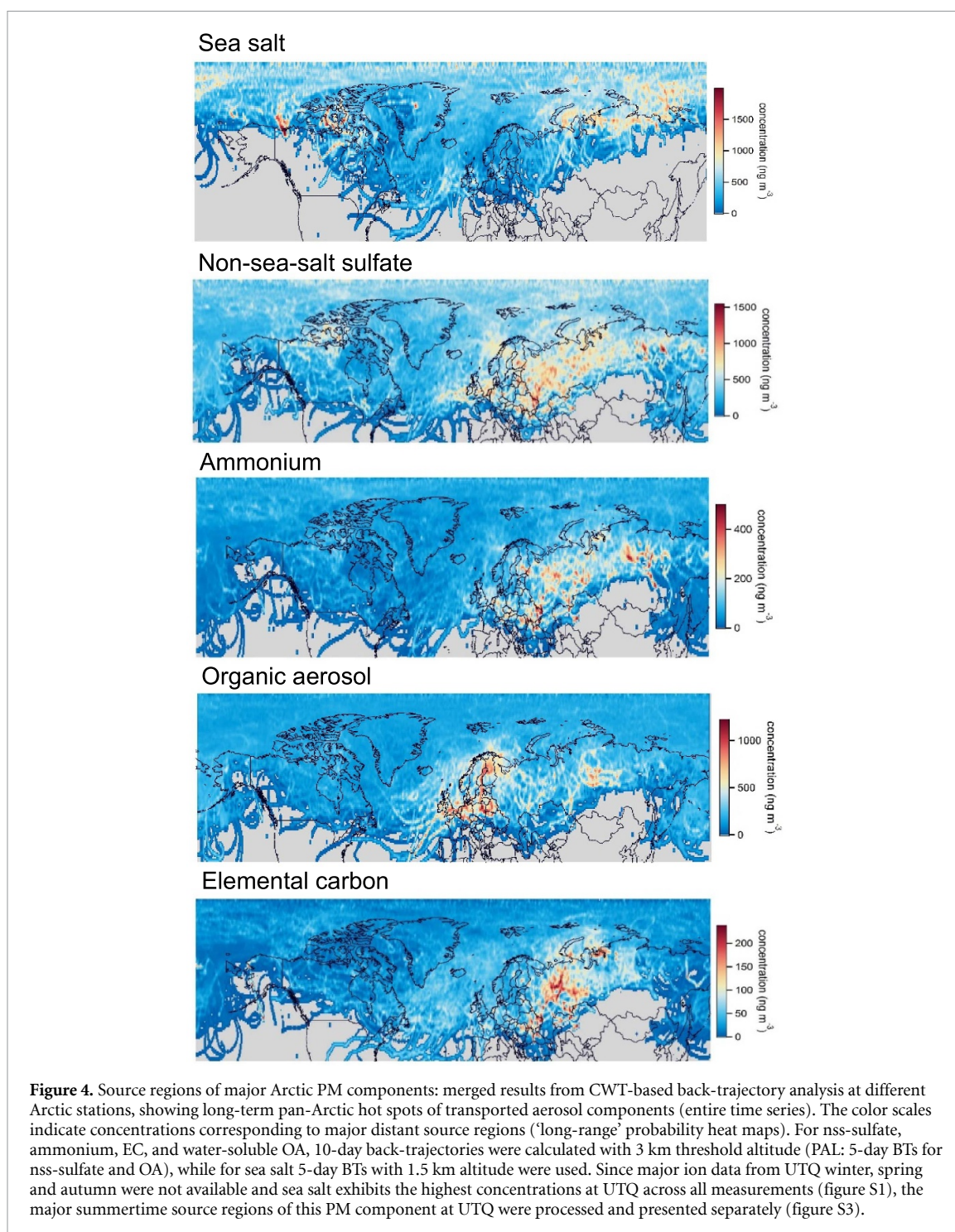
indicates that the ammonium-to-nss-sulfate mass ratio might not always represent the PM acidity in the Arctic but likely only relates to the potential neutrality/acidity of fine-mode particles. The nitrate contribution is rather low (figures 1 and 2), as expected for ammonia-poor acidic or long-range transported (fine-mode) aerosols (Kerminen *et al* 2001, Bauer *et al* 2007, Kim *et al* 2014, Kakavas *et al* 2021).

Total OA contributes on average 22% (Q_1–Q_3 = 11%–28%) to PM (figure 2), which is often comparable to the relative contributions of sea salt and nss-sulfate (figure 1). The hotspot source regions for long-range transported total OA (figure 4), dominated by the highest concentrations at BAR and PAL (up to 1.5 μg m^{-3}; figure S1), are collocated with urban/industrial centers in Europe and West Siberia,

as well as biogenic emission-related regions, such as the Atlantic Ocean and the boreal forests in North-East Europe and central Siberia. That is because OA is a diverse mixture of multiple terrestrial or marine natural and anthropogenic source components in summer and winter (Moschos *et al* 2022). The mean pan-Arctic OA/nss-sulfate ratio (figure 2) is 0.81 (median: 0.63; Q_1–Q_3 = 0.37–1.02). Increased values of 1.20 (median: 0.99; Q_1–Q_3 = 0.75–1.63) are observed at BAR and TIK (figure 2) as well as in general in summer and early autumn (figure 3) when anthropogenic influence is at a minimum (Anthr-OA/OA in figure 3). Similar to our finding, a mean value of the modelled OA/sulfate mass ratio of 0.95 (median: 0.77; inter-model range: 0.25–2.0) has been reported in an evaluation and inter-comparison of

Figure 4. Source regions of major Arctic PM components: merged results from CWT-based back-trajectory analysis at different Arctic stations, showing long-term pan-Arctic hot spots of transported aerosol components (entire time series). The color scales indicate concentrations corresponding to major distant source regions ('long-range' probability heat maps). For nss-sulfate, ammonium, EC, and water-soluble OA, 10-day back-trajectories were calculated with 3 km threshold altitude (PAL: 5-day BTs for nss-sulfate and OA), while for sea salt 5-day BTs with 1.5 km altitude were used. Since major ion data from UTQ winter, spring and autumn were not available and sea salt exhibits the highest concentrations at UTQ across all measurements (figure S1), the major summertime source regions of this PM component at UTQ were processed and presented separately (figure S3).

OA in global (AeroCom phase II) models for the year 2006 (Tsigaridis *et al* 2014). Our OA/nss-sulfate ratio at the different sites and months can be used to constrain the OA budget and seasonality at different Arctic sectors, because sulfate is routinely measured at most observatories included in this study and thus the nss-sulfate budget could be approximated.

The MSA-OA/nss-sulfate ratio (figure 2) peaks in summer (figure 3), reaching up to 0.6 at BAR, GRU, and VRS. Specifically, 6% and 13% of the pan-Arctic values in April–September are >0.4 and >0.2, respectively. Despite being strongly dependent

on temperature and the occurrence of blooms (Yu *et al* 2021), we expect the variability in this ratio to be largely affected by different degrees of anthropogenic perturbation (Kerminen *et al* 1997). Hence, this ratio can be used -indirectly- to distinguish between anthropogenic and natural (marine biogenic) sulfate at different Arctic sectors. The maxima across the three stations (BAR, GRU, and VRS) are comparable to previously reported values at ALT and UTQ (Li and Barrie 1993, Li *et al* 1993). At the same time, the relatively lower maximum summertime value of 0.068 at PAL in May (figure 2), which indicates some Arctic

spatial variability in this ratio, is similar to the value of 0.090 reported for July at Kevo (Laing *et al* 2013), which is located also in the Finnish Arctic. This lower ratio for PAL, indicating a smaller influence of marine MSA in comparison to other stations, can be attributed to its distance to the ocean (>200 km), as well as the predominance of more local aerosol sources (Hellén *et al* 2020) and the advection of air masses of terrestrial origin from lower latitudes (as indicated from the BT analysis) containing nss-sulfate.

The EC relative contribution is on average only 2% of the PM (Q_1–Q_3 = 1%–3%) across the Arctic (figure 2) with no clear seasonal variability (figure 3). We observe enhanced contributions of up to 10% (in individual samples) at BAR and PAL, corresponding to annual mean absolute concentrations (figure S1) of $\sim$90 ng m^{-3} (Q_1–Q_3 = 40–110 ng m^{-3}), and a similarly high median concentration of $\sim$50 ng m^{-3} (Q_1–Q_3 = 30–80 ng m^{-3}) at TIK (figure S1). The higher absolute concentrations at lower latitude Eurasian stations, as well as in winter vs. summer (pan-Arctic mean: 51 vs 19 ng m^{-3}; figure S2), highlight the anthropogenic, predominantly fossil origin (Winiger *et al* 2019) of this component. The median pan-Arctic EC/OA ratio (figure 2) is 0.070 (Q_1–Q_3 = 0.027–0.16), increases in winter (November–March; figure 3), and is highest at BAR and PAL (figure 2). This mass ratio can assist in constraining the absorbing carbonaceous aerosol (brown and BC) radiative effects across the Arctic if the source-specific optical properties are known (Moschos *et al* 2018, Moschos *et al* 2021). The hotspot source regions for EC (figure 4), dominated by the highest concentrations at BAR (up to 350 ng m^{-3}; figure S1), are collocated with West Siberian regions associated with intense gas flaring activity in winter, similar to those found for primary anthropogenic organics (Moschos *et al* 2022). Our multi-site observation agrees with previous single-site studies using trajectory statistics or other transport model calculations. These have attributed winter/spring-high BC levels at ALT, BAR, TIK, UTQ, or ZEP to high-latitude Eurasian (rather than North American or South Asian) source regions (Polissar *et al* 2001, Sharma *et al* 2006, Shindell *et al* 2008, Eleftheriadis *et al* 2009, AMAP 2011, Cheng 2014, Popovicheva *et al* 2019, Manousakas *et al* 2020).

4. Conclusion

Knowing the overall aerosol chemical composition in the Arctic is not only the gateway to differentiating natural from anthropogenic contributions, but also understanding the impact the fast-changing Arctic environment has on the atmospheric chemical composition, and resulting climate feedbacks on the composition, which in turn affect aerosol-radiation and aerosol-cloud interactions. The presented Arctic dataset contains unprecedented comprehensive chemical information from eight Arctic stations for

2014–2019, including individual and comparable anthropogenic and natural component contributions to PM$_{10}$ and TSP dry mass. Our pan-Arctic yearly analyses, including the relative contribution of Arctic organics to PM, their importance compared to secondary inorganics and total carbonaceous aerosols, as well as the ionic balance and seasonal cycle of anions and cations (figure S4; table S1), provide added value compared to earlier studies (e.g. Barrie 1995, Willis *et al* 2018). We show that the major primary (sea salt) and secondary (nss-sulfate) inorganic aerosol components typically dominate the present-day Arctic PM$_{10}$ and TSP mass, especially in winter and at the most remote stations. We demonstrate that the higher PM in spring vs summer (figure S2) is attributed to the seasonal cycle of inorganic components, whereas organics exhibit less of a seasonal cycle in absolute terms (figure S2), as discussed in Moschos *et al* (2022). The increased abundance of sea salt in winter is attributed mainly to blowing snow, whereas the increased abundance of nss-sulfate in spring is attributed to the Arctic haze phenomenon. The spatially and seasonally variable component ratios provide a broader assessment compared to single-component or single-site/season reporting, and hence useful insights for policymakers regarding the yearly relative importance of major aerosol components and sources across the Arctic land surface. We note that a biomass-burning signature might not necessarily be observed at the surface sites investigated here but further aloft (Stohl 2006).

We further examined possible links to regional and distant sources: due to long-range transport of air masses, aerosol particles from the continental Arctic (Eurasia) spread over thousands of kilometers and can influence the radiative balance and the Arctic climate. New insights become available for Siberia from where most of the inner-Arctic air pollution originates. That is illustrated by the high levels of anthropogenic aerosol components (nss-sulfate, EC, Anthr-OA) measured at BAR and TIK combined with the component-specific BT analysis. Our observational effort, extending beyond the traditionally considered BC and sulfate, points to areas that require new measurements (e.g. design of targeted fieldwork) and can support informed policy decisions towards targeted emission reductions (e.g. gas flaring in West Siberia). In addition, models have been struggling to represent the climate change-sensitive natural Arctic aerosol components, such as sea salt and biogenic sulfate/organics. Our holistic observational approach reveals their present-day major source regions for the first time from a pan-Arctic perspective, providing vital information for models to ingest to simulate future Arctic change.

The reported observational results are of general interest to researchers not only focused on Arctic aerosol processes but also on improving model representations of climate-relevant aerosols at the poles

and globally. The findings on speciated natural and anthropogenic aerosol components, including their spatial and seasonal variability and source regions, will be crucial in guiding Arctic climate model evaluation, even though the model spatial resolution remains coarser than that of ground-based point observations. Specifically, the presented complete dataset can assist in reducing uncertainties in Arctic aerosol-climate interaction simulations by constraining the aerosol acidity and hygroscopicity (including the bulk kappa value), carbonaceous aerosol radiative effects, the mass concentration of natural vs. anthropogenic components, and the OA contribution as a function of the better-known nss-sulfate loading. Correlations between components might indicate their mixing state, allowing to constrain radiative effect calculations for Arctic aerosol particles consisting of various components with distinct properties, e.g. OA-coated sea salt in sea spray aerosols (Kirpes *et al* 2019) or internally mixed EC/OA/nss-sulfate in haze particles. While information on the CCN number is not available, model vs. measurement comparisons of the mass concentration of different species and their seasonality is very helpful to validate modelling efforts extending to the entire Arctic and for different seasons. Our dataset is a crucial, timely addition to the upcoming Arctic Monitoring & Assessment Programme (AMAP) report on 'Impacts-of-SLCFs-on-Arctic-Climate-Air-Quality-and-Human-Health', and can further assist in interpreting optical and other polar measurements, e.g. from the year-long MOSAiC expedition in the central Arctic Ocean (Shupe *et al* 2020), in light of the complex aerosol chemistry. It also provides the basis to predict the future evolution of inner-Arctic atmospheric PM, considering rapid environmental changes and emission control measures, by utilizing component-specific decadal trend analyses and applying compound ratios. At the same time, the long-term pan-Arctic aerosol historical trends (Schmale *et al* 2021a) and vertical distribution, including in-cloud processes (Creamean *et al* 2021), remain to be elucidated.

Harmonized, consistent, and comparable yearly measurements, similar to those presented here, should be expanded in the future, e.g. to non-coastal stations closer to the Arctic Circle. While a further decline in anthropogenic-dominated emissions will 'support the implementation of effective measures to reduce local air pollution in Arctic communities', as recommended by AMAP, concurrent aerosol radiative forcing estimates remain uncertain and should be defined more clearly at different Arctic sectors and seasons. Such estimates can only be accurate if atmospheric organics and sea salt are considered, and not only BC and sulfate as is typically the case.

Author contributions

IeH, J S, U B, and V M conceived the study. V M analyzed the data. IeH, J S, A S H P, and U B supported and supervised the research. V M, IeH, J S, and U B interpreted the results. V M, J S, and IeH prepared the figures and wrote the manuscript. L H is the scientific authority for filter sampling, the measurements of EC/OC at ALT (2015–2018), and the data processing/QAQC. W Z performed EC/OC analysis and logistic support for filter sampling at ALT. S S provided the ion chromatography data from ALT 2015–2018. O P coordinated filter sampling and provided ion data from BAR and TIK. S B, G C, M S, R T took care of aerosol samplings at GRU and RT is responsible for the RIS (Research in Svalbard) 3693 project involving multiple aerosol studies at GRU. M V set up and took care of the filter sampling system at PAL. R J S and C E M organized and managed the collection at UTQ. C E M performed ion chromatography for UTQ. A M coordinated the filter sampling at VRS. JKN has analyzed and quality assured the OC/EC data from VRS. H S is the scientific head of VRS and the PI on the research projects that funded the collection of the filters. K E Y and W A A are responsible for the collection of aerosol filter samples at ZEP. J L J contributed with measurements of chemical species on filters using ion chromatography, HPLC-PAD, and HPLC-MS. All co-authors commented on the manuscript.

Conflict of interest

The authors declare that they have no conflict of interest.

ORCID iDs

Vaios Moschos https://orcid.org/0000-0002-6251-4117
Julia Schmale https://orcid.org/0000-0002-1048-7962
Wenche Aas https://orcid.org/0000-0002-2908-1970
Giulia Calzolai https://orcid.org/0000-0002-9476-1470
Konstantinos Eleftheriadis https://orcid.org/0000-0003-2265-4905
Lin Huang https://orcid.org/0000-0002-8200-4632

References

Acosta Navarro J C, Varma V, Riipinen I, Seland Ø, Kirkevåg A, Struthers H, Iversen T, Hansson H C and Ekman A M L 2016 Amplification of Arctic warming by past air pollution reductions in Europe *Nat. Geosci.* **9** 277–81

Adachi K, Oshima N, Ohata S, Yoshida A, Moteki N and Koike M 2021 Compositions and mixing states of aerosol particles by aircraft observations in the Arctic springtime, 2018 *Atmos. Chem. Phys.* **21** 3607–26

AMAP 2015 AMAP assessment 2015: black carbon and ozone as Arctic climate forcers *Arctic Monitoring and Assessment Programme (AMAP)* (Oslo, Norway) pp vii + 116

AMAP 2011 The impact of black carbon on Arctic climate *Arctic Monitoring and Assessment Programme* ed P K Quinn (Oslo: AMAP) p 72

Arnold S R *et al* 2016 Arctic air pollution: challenges and opportunities for the next decade *Elementa* **4** 000104

Barrie L A 1995 Arctic aerosols: composition, sources and transport *Ice Core Studies of Global Biogeochemical Cycles* NATO ASI series (Series I: Global environmental change) vol **30**, ed R J Delmas (Berlin: Springer) (http://doi.org/10.1007/978-3-642-51172-1_1)

Bauer S E, Koch D, Unger N, Metzger S M, Shindell D T and Streets D G 2007 Nitrate aerosols today and in 2030: a global simulation including aerosols and tropospheric ozone *Atmos. Chem. Phys.* **7** 5043–59

Block K, Schneider F A, Mülmenstädt J, Salzmann M and Quaas J 2019 Climate models disagree on the sign of total radiative feedback in the Arctic *Tellus A* **72** 1–14

Cavalli F, Viana M, Yttri K E, Genberg J and Putaud J-P 2010 Toward a standardised thermal-optical protocol for measuring atmospheric organic and elemental carbon: the EUSAAR protocol *Atmos. Meas. Tech.* **3** 79–89

Cheng M-D 2014 Geolocating Russian sources for Arctic black carbon *Atmos. Environ.* **92** 398–410

Cho M-H, Park R J, Yoon J, Choi Y, Jeong J I, Labzovskii L, Fu J S, Huang K, Jeong S-J and Kim B-M 2019 A missing component of Arctic warming: black carbon from gas flaring *Environ. Res. Lett.* **14** 094011

Cohen J *et al* 2014 Recent Arctic amplification and extreme mid-latitude weather *Nat. Geosci.* **7** 627–37

Cohen J *et al* 2018 Arctic change and possible influence on mid-latitude climate and weather: a US CLIVAR white paper *US CLIVAR Rep.* (https://doi.org/10.5065/D6TH8KGW)

Collaud Coen M *et al* 2020 Multidecadal trend analysis of *in situ* aerosol radiative properties around the world *Atmos. Chem. Phys.* **20** 8867–908

Creamean J M, de Boer G, Telg H, Mei F, Dexheimer D, Shupe M D, Solomon A and McComiskey A 2021 Assessing the vertical structure of Arctic aerosols using balloon-borne measurements *Atmos. Chem. Phys.* **21** 1737–57

Curry J A and Ebert E E 1992 Annual cycle of radiation fluxes over the Arctic Ocean: sensitivity to cloud optical properties *J. Clim.* **5** 1267–80

Daellenbach K R *et al* 2016 Characterisation and source apportionment of organic aerosol using offline aerosol mass spectrometry *Atmos. Meas. Tech.* **9** 23–39

Dobricic S, Pozzoli L, Vignati E, Van Dingenen R, Wilson J, Russo S and Klimont Z 2019 Nonlinear impacts of future anthropogenic aerosol emissions on Arctic warming *Environ. Res. Lett.* **14** 034009

Eleftheriadis K, Vratolis S and Nyeki S 2009 Aerosol black carbon in the European Arctic: measurements at Zeppelin station, Ny-Ålesund, Svalbard from 1998-2007 *Geophys. Res. Lett.* **36** L02809

Groot Zwaaftink C D, Grythe H, Skov H and Stohl A 2016 Substantial contribution of northern high-latitude sources to mineral dust in the Arctic *J. Geophys. Res. Atmos.* **121** 13678–97

Han Y-J, Holsen T M and Hopke P K 2007 Estimation of source locations of total gaseous mercury measured in New York State using trajectory-based models *Atmos. Environ.* **41** 6033–47

Hegerl G C, Brönnimann S, Cowan T, Friedman A R, Hawkins E, Iles C, Müller W, Schurer A and Undorf S 2019 Causes of climate change over the historical record *Environ. Res. Lett.* **14** 123006

Hellén H, Schallhart S, Praplan A P, Tykkä T, Aurela M, Lohila A and Hakola H 2020 Sesquiterpenes dominate monoterpenes in northern wetland emissions *Atmos. Chem. Phys.* **20** 7021–34

Hirdman D, Burkhart J F, Sodemann H, Eckhardt S, Jefferson A, Quinn P K, Sharma S, Ström J and Stohl A 2010 Long-term trends of black carbon and sulphate aerosol in the Arctic: changes in atmospheric transport and source region emissions *Atmos. Chem. Phys.* **10** 9351–68

Huang J and Jaeglé L 2017 Wintertime enhancements of sea salt aerosol in polar regions consistent with a sea ice source from blowing snow *Atmos. Chem. Phys.* **17** 3699–712

Huang L, Zhang W, Santos G M, Rodríguez B T, Holden S R, Vetro V and Czimczik C I 2021 Application of the ECT9 protocol for radiocarbon-based source apportionment of carbonaceous aerosols *Atmos. Meas. Tech.* **14** 3481–500

IPCC: Climate Change 2013 2013 The physical science basis *Contribution of Working Group I to the Fifth Assessment Report of the Intergovernmental Panel on Climate Change* (Cambridge: Cambridge University) p 1535

IPCC: Climate Change 2021 The physical science basis *Contribution of Working Group I to the Sixth Assessment Report of the Intergovernmental Panel on Climate Change* (Cambridge University Press) accepted

Jaffrezo J-L, Calas N and Bouchet M 1998 Carboxylic acids measurements with ionic chromatography *Atmos. Environ.* **32** 2705–8

Kakavas S, Patoulias D, Zakoura M, Nenes A and Pandis S N 2021 Size-resolved aerosol pH over Europe during summer *Atmos. Chem. Phys.* **21** 799–811

Kerminen V-M, Aurela M, Hillamo R E and Virkkula A 1997 Formation of particulate MSA: deductions from size distribution measurements in the Finnish Arctic *Tellus* B **49** 159–71

Kerminen V-M, Hillamo R, Teinilä K, Pakkanen T, Allegrini I and Sparapani R 2001 Ion balances of size-resolved tropospheric aerosol samples: implications for the acidity and

atmospheric processing of aerosols *Atmos. Environ.* **35** 5255–65

Kim Y J, Spak S N, Carmichael G R, Riemer N and Stanier C O 2014 Modeled aerosol nitrate formation pathways during wintertime in the Great Lakes region of North America *J. Geophys. Res. Atmos.* **119** 12,420–412,445

Kirkevåg A *et al* 2013 Aerosol–climate interactions in the Norwegian earth system model—NorESM1-M *Geosci. Mod. Dev.* **6** 207–44

Kirpes R M, Bonanno D, May N W, Fraund M, Barget A J, Moffet R C, Ault A P and Pratt K A 2019 Wintertime Arctic sea spray aerosol composition controlled by sea ice lead microbiology *ACS Cent. Sci.* **5** 1760–7

Kulmala M 2018 Build a global Earth observatory *Nature* **553** 21–23

Kyrö E M *et al* 2014 Trends in new particle formation in eastern Lapland, Finland: effect of decreasing sulfur emissions from Kola peninsula *Atmos. Chem. Phys.* **14** 4383–96

Laing J R, Hopke P K, Hopke E F, Husain L, Dutkiewicz V A, Paatero J and Viisanen Y 2013 Long-term trends of biogenic sulfur aerosol and its relationship with sea surface temperature in Arctic Finland *J. Geophys. Res. Atmos.* **118** 11770–6

Lange R, Dall'Osto M, Wex H, Skov H and Massling A 2019 Large summer contribution of organic biogenic aerosols to Arctic cloud condensation nuclei *Geophys. Res. Lett.* **46** 11500–9

Leaitch W R, Russell L M, Liu J, Kolonjari F, Toom D, Huang L, Sharma S, Chivulescu A, Veber D and Zhang W 2018 Organic functional groups in the submicron aerosol at 82.5° N, 62.5° W from 2012 to 2014 *Atmos. Chem. Phys.* **18** 3269–87

Li S-M and Barrie L A 1993 Biogenic sulfur aerosol in the Arctic troposphere: 1. Contributions to total sulfate *J. Geophys. Res. Atmos.* **98** 20613–22

Li S-M, Barrie L A, Talbot R W, Harriss R C, Davidson C I and Jaffrezo J-L 1993 Seasonal and geographic variations of methanesulfonic acid in the Arctic troposphere *Atmos. Environ.* **27** 3011–24

Liu X and Wang J 2010 How important is organic aerosol hygroscopicity to aerosol indirect forcing? *Environ. Res. Lett.* **5** 044010

Liu Y and Key J R 2014 Less winter cloud aids summer 2013 Arctic sea ice return from 2012 minimum *Environ. Res. Lett.* **9** 044002

Lohmann U, Friebel F, Kanji Z A, Mahrt F, Mensah A A and Neubauer D 2020 Future warming exacerbated by aged-soot effect on cloud formation *Nat. Geosci.* **13** 674–80

Lubin D and Vogelmann A M 2006 A climatologically significant aerosol longwave indirect effect in the Arctic *Nature* **439** 453–6

Mann G W *et al* 2014 Intercomparison and evaluation of global aerosol microphysical properties among AeroCom models of a range of complexity *Atmos. Chem. Phys.* **14** 4679–713

Manousakas M, Popovicheva O, Evangeliou N, Diapouli E, Sitnikov N, Shonija N and Eleftheriadis K 2020 Aerosol carbonaceous, elemental and ionic composition variability and origin at the Siberian High Arctic, Cape Baranova *Tellus* B **72** 1–14

Masiol M *et al* 2020 Hybrid multiple-site mass closure and source apportionment of PM$_{2.5}$ and aerosol acidity at major cities in the Po Valley *Sci. Total Environ.* **704** 135287

Mauritsen T *et al* 2011 An Arctic CCN-limited cloud-aerosol regime *Atmos. Chem. Phys.* **11** 165–73

Menon S, Unger N, Koch D, Francis J, Garrett T, Sednev I, Shindell D and Streets D 2008 Aerosol climate effects and air quality impacts from 1980 to 2030 *Environ. Res. Lett.* **3** 024004

Moffett C E, Barrett T E, Liu J, Gunsch M J, Upchurch L M, Quinn P K, Pratt K A and Sheesley R J 2020 Long-term trends for marine sulfur aerosol in the Alaskan Arctic and relationships with temperature *J. Geophys. Res. Atmos.* **125** D033225

Moschos V 2021 Dataset for elucidating the present-day chemical composition, seasonality and source regions of climate-relevant aerosols across the Arctic land surface (https://doi.org/10.5281/zenodo.5179984) (Accessed 11 August 2021)

Moschos V *et al* 2021 Source-specific light absorption by carbonaceous components in the complex aerosol matrix from yearly filter-based measurements *Atmos. Chem. Phys.* **21** 12809–33

Moschos V *et al* 2022 Equal abundance of summertime natural and wintertime anthropogenic Arctic organic aerosols *Nat. Geosci.* (https://doi.org/10.1038/s41561-021-00891-1)

Moschos V, Kumar N K, Daellenbach K R, Baltensperger U, Prévôt A S H and El Haddad I 2018 Source apportionment of brown carbon absorption by coupling ultraviolet–visible spectroscopy with aerosol mass spectrometry *Environ. Sci. Technol. Lett.* **5** 302–8

Najafi M R, Zwiers F W and Gillett N P 2015 Attribution of Arctic temperature change to greenhouse-gas and aerosol influences *Nat. Clim. Change* **5** 246–9

Nguyen Q T, Kjær K H, Kling K I, Boesen T and Bilde M 2017 Impact of fatty acid coating on the CCN activity of sea salt particles *Tellus B: Chem. Phys. Met.* **69** 1304064

Norman A L, Barrie L A, Toom-Sauntry D, Sirois A, Krouse H R, Li S M and Sharma S 1999 Sources of aerosol sulphate at Alert: apportionment using stable isotopes *J. Geophys. Res. Atmos.* **104** 11619–31

Petäjä T *et al* 2020 Overview: integrative and comprehensive understanding on polar environments (iCUPE)—concept and initial results *Atmos. Chem. Phys.* **20** 8551–92

Petit J E, Favez O, Albinet A and Canonaco F 2017 A user-friendly tool for comprehensive evaluation of the geographical origins of atmospheric pollution: wind and trajectory analyses *Environ. Model. Softw.* **88** 183–7

Pithan F and Mauritsen T 2014 Arctic amplification dominated by temperature feedbacks in contemporary climate models *Nat. Geosci.* **7** 181–4

Polissar A V, Hopke P K and Harris J M 2001 Source regions for atmospheric aerosol measured at Barrow, Alaska *Environ. Sci. Technol.* **35** 4214–26

Popovicheva O B, Evangeliou N, Eleftheriadis K, Kalogridis A C, Sitnikov N, Eckhardt S and Stohl A 2017 Black carbon sources constrained by observations in the Russian High Arctic *Environ. Sci. Technol.* **51** 3871–9

Popovicheva O, Diapouli E, Makshtas A, Shonija N, Manousakas M, Saraga D, Uttal T and Eleftheriadis K 2019 East Siberian Arctic background and black carbon polluted aerosols at HMO Tiksi *Sci. Total Environ.* **655** 924–38

Qian Y, Wang H, Zhang R, Flanner M G and Rasch P J 2014 : a sensitivity study on modeling black carbon in snow and its radiative forcing over the Arctic and Northern China *Environ. Res. Lett.* **9** 064001

Quinn P K, Miller T L, Bates T S, Ogren J A, Andrews E and Shaw G E 2002 A 3-year record of simultaneously measured aerosol chemical and optical properties at Barrow, Alaska *J. Geophys. Res. Atmos.* **107** AAC 8-1-AAC 8-15

Quinn P K, Shaw G, Andrews E, Dutton E G, Ruoho-Airola T and Gong S L 2007 Arctic haze: current trends and knowledge gaps *Tellus* B **59** 99–114

Rai P *et al* 2020 Real-time measurement and source apportionment of elements in Delhi's atmosphere *Sci. Total Environ.* **742** 140332

Ren L, Yang Y, Wang H, Zhang R, Wang P and Liao H 2020 Source attribution of Arctic black carbon and sulfate aerosols and associated Arctic surface warming during 1980–2018 *Atmos. Chem. Phys.* **20** 9067–85

Sand M, Berntsen T K, Von Salzen K, Flanner M G, Langner J and Victor D G 2015 Response of Arctic temperature to changes in emissions of short-lived climate forcers *Nat. Clim. Change* **6** 286–9

Sand M *et al* 2017 Aerosols at the poles: an AeroCom phase II multi-model evaluation *Atmos. Chem. Phys.* **17** 12197–218

Schmale J, Arnold S R, Law K S, Thorp T, Anenberg S, Simpson W R, Mao J and Pratt K A 2018 Local Arctic air pollution: a neglected but serious problem *Earth's Future* **6** 1385–412

Schmale J *et al* 2021a Pan-Arctic seasonal cycles and long-term trends of aerosol properties from ten observatories *Atmos. Chem. Phys. Discuss.* (https://doi.org/10.5194/acp-2021-756)

Schmale J, Zieger P and Ekman A M L 2021b Aerosols in current and future Arctic climate *Nat. Clim. Change* **11** 95–105

Schneider J *et al* 2021 The seasonal cycle of ice-nucleating particles linked to the abundance of biogenic aerosol in boreal forests *Atmos. Chem. Phys.* **21** 3899–918

Serreze M C and Barry R G 2011 Processes and impacts of Arctic amplification: a research synthesis *Glob. Planet. Change* **77** 85–96

Sharma S, Andrews E, Barrie L A, Ogren J A and Lavoué D 2006 Variations and sources of the equivalent black carbon in the High Arctic revealed by long-term observations at Alert and Barrow: 1989–2003 *J. Geophys. Res. Atmos.* **111** D14208

Sharma S, Barrie L A, Magnusson E, Brattström G, Leaitch W R, Steffen A and Landsberger S 2019 A factor and trends analysis of multidecadal lower tropospheric observations of Arctic aerosol composition, black carbon, ozone, and mercury at Alert, Canada *J. Geophys. Res. Atmos.* **124** 14133–61

Shindell D T *et al* 2008 A multi-model assessment of pollution transport to the Arctic *Atmos. Chem. Phys.* **8** 5353–72

Shindell D and Faluvegi G 2009 Climate response to regional radiative forcing during the twentieth century *Nat. Geosci.* **2** 294–300

Shupe M D *et al* 2020 The MOSAiC expedition: a year drifting with the Arctic sea ice *NOAA Arctic Report Card* (https://doi.org/10.25923/9g3v-xh92)

Shupe M D and Intrieri J M 2004 Cloud radiative forcing of the Arctic surface: the influence of cloud properties, surface albedo, and solar zenith angle *J. Clim.* **17** 616–28

Sirois A and Barrie L A 1999 Arctic lower tropospheric aerosol trends and composition at Alert, Canada: 1980-1995 *J. Geophys. Res. Atmos.* **104** 11599–618

Stohl A 2006 Characteristics of atmospheric transport into the Arctic troposphere *J. Geophys. Res. Atmos.* **111** D11306

Struthers H, Ekman A M L, Glantz P, Iversen T, Kirkevåg A, Mårtensson E M, Seland Ø and Nilsson E D 2011 The effect of sea ice loss on sea salt aerosol concentrations and the radiative balance in the Arctic *Atmos. Chem. Phys.* **11** 3459–77

Tan I and Storelvmo T 2019 Evidence of strong contributions from mixed-phase clouds to Arctic climate change *Geophys. Res. Lett.* **46** 2894–902

Tong H *et al* 2021 Aqueous-phase reactive species formed by fine particulate matter from remote forests and polluted urban air *Atmos. Chem. Phys.* **21** 10439–55

Tsigaridis K *et al* 2014 The AeroCom evaluation and intercomparison of organic aerosol in global models *Atmos. Chem. Phys.* **14** 10845–95

Udisti R *et al* 2016 Sulfate source apportionment in the Ny-Ålesund (Svalbard Islands) Arctic aerosol *Rend. Fis. Acc. Lincei* **27** 85–94

Uttal T *et al* 2016 International Arctic systems for observing the atmosphere: an international polar year legacy consortium *Bull. Am. Meteorol. Soc.* **97** 1033–56

Wang M Y *et al* 2020 Photo-oxidation of aromatic hydrocarbons produces low-volatility organic compounds *Environ. Sci. Technol.* **54** 7911–21

Wang Y, Jiang J H, Su H, Choi Y-S, Huang L, Guo J and Yung Y L, 2018 Elucidating the role of anthropogenic aerosols in Arctic sea ice variations *J. Clim.* **31** 99–114

Wegmann M, Orsolini Y and Zolina O 2018 Warm Arctic—
cold Siberia: comparing the recent and the early
20th-century Arctic warmings *Environ. Res. Lett.*
13 025009

Willis M D, Leaitch W R and Abbatt J P D 2018 Processes
controlling the composition and abundance of Arctic
aerosol *Rev. Geophys.* **56** 621–71

Winiger P *et al* 2019 Source apportionment of
circum-Arctic atmospheric black carbon from
isotopes and modeling *Sci. Adv.*
5 eaau8052

Xu J *et al* 2020 An interlaboratory comparison of aerosol
inorganic ion measurements by ion chromatography:
implications for aerosol pH estimate *Atmos. Meas. Tech.*
13 6325–41

Yang Q, Bitz C M and Doherty S J 2014 Offsetting effects of
aerosols on Arctic and global climate in the late 20th century
Atmos. Chem. Phys. **14** 3969–75

Yu C, Yan J, Zhang H, Lin Q, Zheng H, Zhao S, Zhong X, Zhao S,
Zhang M and Chen L 2021 Chemical characteristics of
sulfur-containing aerosol particles across the western North
Pacific and the Arctic Ocean *Atmosp. Res.* **253** 105480